

# jXBW: Fast Substructure Search for Large-Scale JSONL Datasets with LLM Applications

Yasuo Tabei

yasuo.tabei@riken.jp

RIKEN Center for Advanced Intelligence Project  
Tokyo, Japan

## ABSTRACT

JSON Lines (JSONL) has become a popular format for managing large collections of semi-structured data, from *large language model (LLM) prompts* to chemical compound records and geospatial datasets. A key operation in this setting is *substructure search*, where the goal is to identify all JSON objects that contain a given query pattern. Substructure search underpins applications such as drug discovery (querying compounds for specific functional groups), prompt engineering (extracting prompts with particular schema fragments), and geospatial analytics (finding entities with nested attributes), but existing solutions are impractical: straightforward traversal requires exhaustive tree matching, succinct JSON representations save space but do not accelerate search, and XML-based approaches add conversion overhead and semantic mismatches. We propose **jXBW**, a compressed index for fast substructure search over JSONL. jXBW combines three innovations: (i) a merged tree representation that consolidates repeated structures across objects, (ii) a succinct tree index based on the eXtended Burrows–Wheeler Transform (XBW), and (iii) a three-phase algorithm for efficient substructure search. Together, these techniques achieve **query-dependent complexity**, where the cost is determined by query characteristics rather than dataset size, while maintaining succinct space usage. This addresses a critical bottleneck in retrieval-augmented generation (RAG) systems that require structure-aware retrieval over semi-structured data. Experiments on seven real-world datasets, including PubChem (1M compounds) and OSM geospatial data (6.6M objects), demonstrate up to **4,700× speedup** over tree-based methods and over  $6 \times 10^6$  **speedup** compared to XML-based processing. jXBW thus makes JSONL substructure search practical for the first time, opening up new opportunities for **large-scale LLM-based analytics**.

## CCS CONCEPTS

- **Information systems** → **Data structures**; *Query processing*;
- **Theory of computation** → *Data compression*; • **Computing methodologies** → *Machine learning*.

---

Permission to make digital or hard copies of all or part of this work for personal or classroom use is granted without fee provided that copies are not made or distributed for profit or commercial advantage and that copies bear this notice and the full citation on the first page. Copyrights for components of this work owned by others than the author(s) must be honored. Abstracting with credit is permitted. To copy otherwise, or republish, to post on servers or to redistribute to lists, requires prior specific permission and/or a fee. Request permissions from [permissions@acm.org](mailto:permissions@acm.org).

*SIGMOD '26, May 31–June 5, 2026, Bengaluru, India*

© 2026 Copyright held by the owner/author(s). Publication rights licensed to ACM. ACM ISBN 978-1-4503-XXXX-X/2026/05...\$15.00  
<https://doi.org/XXXXXXX.XXXXXXX>

## KEYWORDS

XBW Transform, Substructure Search, JSONL, Compressed Data Structure, Large Language Model (LLM), Retrieval-Augmented Generation (RAG)

### ACM Reference Format:

Yasuo Tabei. 2026. jXBW: Fast Substructure Search for Large-Scale JSONL Datasets with LLM Applications. In *2026 International Conference on Management of Data*. ACM, New York, NY, USA, 17 pages. <https://doi.org/XXXXXXX.XXXXXXX>

## 1 INTRODUCTION

JSON Lines (JSONL) is rapidly becoming the *de facto standard* for representing large collections of semi-structured objects. Each line in a JSONL file contains a single, self-contained JSON object, enabling efficient storage and streaming of large datasets. From *large language model (LLM)* prompts in generative AI services to chemical compound records in scientific repositories to OpenStreetMap (OSM) geospatial objects, JSONL offers a lightweight yet expressive way to encode millions of objects. Enterprise applications and research platforms commonly employ the JSONL format to manage complex prompt datasets that can contain millions of structured queries and contextual information [4, 17, 26]. Its simplicity and line-by-line structure make it attractive for data processing pipelines, enterprise logging, and large-scale analytics. The practical importance of JSONL is reinforced by recent work: GPU-accelerated libraries such as NVIDIA cuDF achieve up to **133× speedup** for JSONL ingestion compared to pandas, highlighting the demand for efficient JSONL processing in production workflows [21].

Recent studies also underscore the role of *prompt formats* in LLM performance. He et al. [10] show that the choice of format – JSON versus Markdown – can boost accuracy by as much as **40%** in reasoning tasks. Similarly, Zhang et al. [27] demonstrate that structured JSON prompts outperform YAML or hybrid CSV in GPT-4o, yielding the most reliable results for complex tasks. These findings make clear that structured inputs are not only more efficient but also more accurate, strengthening the case for JSONL as a unifying format for modern AI and data systems.

In enterprise applications, data are often stored across multiple relational databases in normalized form, requiring complex joins to assemble the information needed by downstream applications. While relational databases excel at ensuring consistency, such normalized schemas are not well aligned with language models, which benefit from flattened, object-like representations. A common approach is therefore to transform relational data into JSON objects, enabling easier integration with LLMs. This reflects a broader trend: object databases and modern NoSQL systems (e.g., MongoDB) store

data natively as JSON, offering a natural fit for LLM-based analytics [17, 26]. These considerations further highlight why JSONL has emerged as a practical and widely adopted format for large-scale AI and data science workflows.

Despite its adoption, efficient querying over JSONL remains a **critical bottleneck**. In many applications, the task is not simply to retrieve documents by keyword or field but to identify all objects that contain a given *substructure* (i.e., *substructure search*). Examples include: **Drug discovery**, where chemists must query millions of compounds for molecules containing specific functional groups; **Prompt engineering**, where developers need to extract all prompts containing a particular schema fragment or contextual pattern; **Geospatial analytics**, where analysts search for OSM entities with nested attributes (e.g., convenience stores with parking lots).

Such substructure search queries are **computationally expensive**. Each JSON object can be naturally represented as a tree, making substructure search essentially a *tree-matching problem*. Direct traversal therefore requires exhaustive matching and scales linearly with dataset size. The problem is further complicated by the need to handle both ordered structures (JSON arrays) and unordered structures (JSON objects). Succinct JSON representations such as SJSON [14] reduce memory usage but provide **no acceleration** for substructure queries. Alternatively, one can transform JSON objects into XML and leverage XQuery for substructure search, benefiting from mature XML indexing technologies [3, 24]. However, this approach introduces substantial overhead: the JSON-to-XML conversion process increases data volume and processing latency, while semantic differences between JSON and XML models—particularly in handling arrays, null values, and type distinctions—complicate query formulation and result interpretation. Moreover, this approach requires performing individual substructure searches across numerous XML documents converted from each JSON object, leading to computational overhead that scales linearly with dataset size.

The challenge is particularly pressing in the context of **retrieval-augmented generation (RAG)**. RAG has become a central paradigm for improving factuality in LLMs by injecting retrieved knowledge into the generation process [15]. Yet conventional RAG methods operate on unstructured text chunks, which hinders multi-hop reasoning and global integration. To overcome this, recent work has emphasized *structurization*: Retrieval-And-Structuring (RAS) [12] dynamically builds query-specific knowledge graphs, while StructRAG [16] selects task-appropriate structures such as tables or graphs. These advances share a key insight: **structure is essential for robust reasoning**. However, existing methods focus on natural language documents. For semi-structured data such as JSONL, **no efficient system** supports structure-aware retrieval and reasoning. Therefore, an important open challenge is to develop specialized data structures and algorithms that can efficiently support substructure search directly on JSONL data.

**Our contributions are as follows:**

- We identify the **JSONL substructure search problem** and show why existing JSON/XML indexing approaches fail to address it efficiently.

- We propose **jXBW**, a novel compressed index combining (i) a merged tree representation, (ii) an XBW-based succinct tree index, and (iii) a three-phase substructure search algorithm.
- We provide a **complexity analysis**, showing that jXBW achieves **query-dependent complexity**, determined by query structure rather than dataset size, while keeping space usage succinct.
- We evaluate jXBW on seven real-world JSONL datasets, demonstrating up to **4,700× speedup** over tree-based methods and over **6M× speedup** compared to XML-based processing.

This establishes jXBW as the **first practical solution** for *JSONL substructure search*, opening up new opportunities for **large-scale LLM-based analytics**.

## 2 METHOD

### 2.1 JSONL and its Tree Representation

JSONL is a text-based format in which each line represents a single JSON object composed of key-value pairs. Let a JSONL file consist of  $N$  objects denoted by  $O_i$ , where  $i = 1, 2, \dots, N$ . Formally, each JSON object  $O_i$  can be defined using Backus–Naur Form (BNF) as follows:

```

<object> ::= { <members> ? }
<members> ::= <pair> ( , <pair> )*
<pair> ::= <string> : <value>
Here, <value> may be one of the following: <string>, <number>,
<object>, <array>, true, false, or null.

```

An  $<\text{object}>$  may optionally include  $<\text{members}>$ , which consist of one or more unordered  $<\text{pair}>$  elements. Each  $<\text{pair}>$  represents a key-value association, where the key is a  $<\text{string}>$ , and the value is any valid JSON data type as defined above. An  $<\text{array}>$  represents an ordered sequence of elements, each of which may be of any valid JSON data type.

An example involving two JSON objects that manage information about two individuals, Alice and Bob, is given as follows:

```

01      =      {"person": {"name": "Alice", "age": 30},
               "hobbies": ["reading", "cycling"]}
02      =      {"person": {"name": "Bob", "age": 30},
               "hobbies": ["reading"]}

```

**Tree Representation.** Each object  $O_i$  can be systematically transformed into a tree-based representation with node labels. Let  $T_i$  denote the tree constructed from the  $i$ -th object  $O_i$  and  $|T_i|$  denote the number of nodes in  $T_i$ . The root node of  $T_i$  is labeled “object” and has as many unordered child nodes as there are  $<\text{pair}>$  elements in the  $<\text{members}>$ . If the  $<\text{object}>$  contains no  $<\text{members}>$ , the root node has no children.

Each  $<\text{pair}>$  consists of a key-value association of the form  $<\text{string}>:<\text{value}>$ . In the corresponding tree structure, each child of the root is labeled with the key  $<\text{string}>$  and has a single child node representing the value. The value node may correspond to any valid JSON type:  $<\text{string}>$ ,  $<\text{number}>$ ,  $<\text{object}>$ ,  $<\text{array}>$ , true, false, or null. If the value is an  $<\text{object}>$ , the tree expands recursively, treating the value node as the root of a new subtree. If the value is an  $<\text{array}>$ , the value node has multiple children, each representing an element of the array in the specified order. Each element may itself be of any valid JSON type.

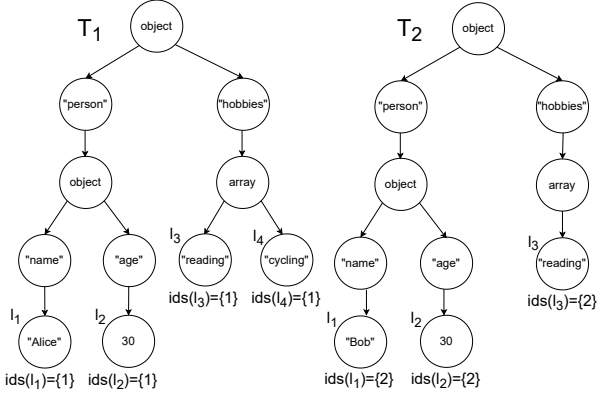


Figure 1: Tree structures  $T_1$  (left) and  $T_2$  (right), derived from the example JSON objects  $O_1$  and  $O_2$ , respectively.

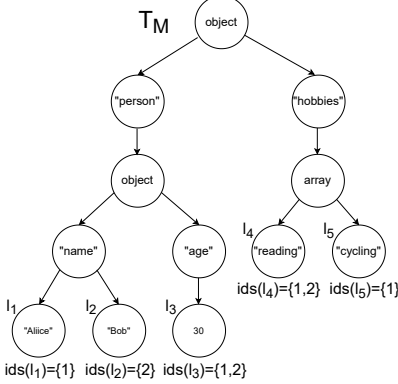


Figure 2: Merged tree  $T_M$  derived from  $T_1$  and  $T_2$ .

Furthermore, each leaf node  $\ell$  in tree  $T_i$  is annotated with the tree identifier  $i$  to track its origin. For any leaf node  $\ell$ , we define  $ids(\ell)$  as the set of all tree identifiers associated with that leaf node. In individual trees, this is simply  $ids(\ell) = \{i\}$  for leaf node  $\ell$  in tree  $T_i$ .

Figure 1 illustrates the tree structures  $T_1$  and  $T_2$  derived from the example JSON objects  $O_1$  and  $O_2$  which describe two individuals: Alice and Bob. The leaf nodes in  $T_1$  and  $T_2$  are annotated with identifiers 1 and 2, respectively.

Our substructure search is formulated as follows.

**Definition 2.1 (Substructure Search Problem).** Consider a set of  $N$  trees  $T_1, T_2, \dots, T_N$ , where each tree  $T_i$  is derived from a JSON object in a JSONL file. The substructure search problem is defined as follows: given a query tree  $Q$ , find all indices  $i \in \{1, 2, \dots, N\}$  such that tree  $T_i$  contains  $Q$  as a substructure. Here,  $Q$  is considered a substructure of  $T_i$  if there exists a mapping from each node in  $Q$  to a node in  $T_i$  such that (i) corresponding nodes have the same label, (ii) the parent-child relationships are preserved, and (iii) the ordering constraints are satisfied according to the JSON semantics:

unordered matching for JSON object children and ordered matching for JSON array children.

The query tree  $Q$  can be derived from any valid JSON structure: JSON objects, JSON arrays, or nested combinations. The algorithm handles different ordering semantics appropriately:

- JSON objects: unordered matching of key-value pairs
- JSON arrays: ordered matching of elements
- Primitive values: exact match under JSON typing (strings, numbers, booleans, and null)

A straightforward approach to substructure search in problem 2.1 would involve searching each individual tree  $T_i$  separately for the query tree  $Q$ . However, this approach has significant computational drawbacks. First, it requires  $O((\sum_{i=1}^N |T_i|) \cdot |Q|)$  time complexity, where  $|T_i|$  is the number of nodes in  $T_i$  and each tree must be traversed independently to find potential matches. Second, this approach fails to exploit structural similarities between trees, resulting in redundant computations when many trees share common substructures. To overcome these limitations, we introduce an efficient merged tree representation that consolidates shared structural patterns while preserving individual tree identities.

### 3 MERGED TREE REPRESENTATION

To address these limitations and enable more efficient substructure queries, we construct a single merged tree by combining the individual trees generated from the input JSONL file. Two trees are said to share a common prefix path from the root if their corresponding nodes at each level along the path have identical labels. Nodes that match in both label and position along such a path are merged into a single node in the merged tree  $T_M$ . When the paths diverge—i.e., when child nodes have different labels—each divergent node continues as a new branch attached to the last shared node on the prefix path.

Each leaf node  $\ell$  in  $T_M$  retains the identifiers of all individual trees  $T_i$  that share the same root-to-leaf path, i.e.,  $ids(\ell) = \{i \mid T_i \text{ has a leaf node reachable through the same sequence of node labels from root to } \ell\}$ . Algorithm 2 in Appendix A presents a pseudo-code for the tree merging algorithm.

An example of the merged tree  $T_M$  derived from  $T_1$  and  $T_2$  is presented in Figure 2. In this example, both the leaf nodes labeled "30" and "reading" are reached through paths shared by  $T_1$  and  $T_2$ , resulting in these leaf nodes  $\ell_3$  and  $\ell_4$  having  $ids(\ell_3) = \{1, 2\}$  and  $ids(\ell_4) = \{1, 2\}$  in the merged tree. The other leaf nodes  $\ell_1$  labeled "Alice",  $\ell_2$  labeled "Bob", and  $\ell_5$  labeled "cycling" have  $ids(\ell_1) = \{1\}$ ,  $ids(\ell_2) = \{2\}$ , and  $ids(\ell_5) = \{1\}$ , respectively.

The merged tree representation provides significant memory efficiency compared to storing individual trees separately. The space complexity of the merged tree is  $O(|T_M|)$ , where  $|T_M| \leq \sum_{i=1}^N |T_i|$  with equality only when no structural patterns are shared among the input trees. In practice, when input trees share common structural patterns—which is typical in real-world JSON datasets—the merged tree achieves substantial space savings with  $|T_M| \ll \sum_{i=1}^N |T_i|$ .

When merging a sequence of  $N$  trees  $T_1, T_2, \dots, T_N$  sequentially, define the total number of nodes as  $M_{\text{tot}} = \sum_{i=1}^N |T_i|$ . In typical cases where node labels are distinct or only partially overlapping, each merge takes  $O(|T| + |T'|)$  time, resulting in a total cost of  $O(M_{\text{tot}} \cdot N)$ .

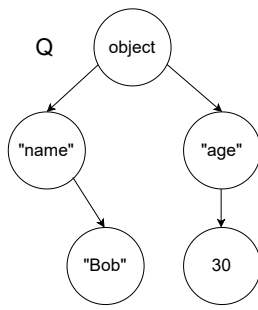


Figure 3: Example query tree structure.

However, in worst-case scenarios where all node labels are identical and tree structures are highly similar, each individual merge may require  $O(|T| \times |T'|)$  time due to the need to examine all possible node pairings, leading to a total cost that can reach  $O(M_{\text{tot}}^2)$ .

**Divide-and-Conquer Strategy.** To address this, we adopt a divide-and-conquer strategy that merges trees in a balanced hierarchical manner. At each level of recursion, trees are paired and merged in parallel, and this process is repeated until a single tree remains. Since the total number of nodes  $M_{\text{tot}}$  remains unchanged throughout the merging process, and each level processes all nodes once, the cost per level is  $O(M_{\text{tot}})$ . As the number of levels is  $O(\log N)$ , the overall merging cost is reduced to  $O(M_{\text{tot}} \log N)$ . This strategy significantly improves efficiency by avoiding the accumulation of large intermediate trees that occurs in sequential merging, and it ensures better scalability when handling a large number of input trees.

### 3.1 Substructure Search on Merged Tree

The substructure search algorithm on the merged tree  $MT$  operates as follows. The algorithm operates by traversing  $MT$  and identifying candidate nodes with the same label as the root of query tree  $Q$ . For each candidate node  $v$ , the algorithm recursively verifies whether the subtree rooted at  $v$  contains a substructure that matches  $Q$ .

The matching process works as follows:

- (1) **Candidate finding:** Finding nodes in  $MT$  with the same label as the root of  $Q$  by traversing  $MT$ .
- (2) **Substructure matching:** For each candidate node  $v$ , recursively check if the subtree rooted at  $v$  matches the structure of query tree  $Q$ . This requires exhaustively comparing the labels of child nodes between corresponding nodes in  $MT$  and  $Q$  to find matches, resulting in computational overhead that is proportional to the product of the branching factors of both the merged tree and query tree nodes. When the search reaches the  $j$ -th leaf node  $\ell_j$  of  $Q$  with  $L$  leaf nodes, collect the stored tree identifiers from the corresponding matched leaf node in  $MT$  and record them in the set  $I(\ell_j)$ .
- (3) **Solution identification:** Compute the intersection of all collected identifier sets  $\bigcap_{j=1}^L I(\ell_j)$  for all leaves  $\ell_1, \ell_2, \dots, \ell_L$  in  $Q$ . This intersection represents the set of original trees that contain  $Q$  as a substructure.

Since each leaf node in the merged tree retains the identifiers of all original trees that contributed to that specific structural path, this approach can identify all trees containing the query as a substructure by leveraging the consolidated structure without requiring individual searches on each original tree.

The detailed algorithms for substructure search on merged tree are provided in Appendix B.

For the example query object  $\{\text{"name"} : \text{"Bob"}, \text{"age"} : 30\}$ , we convert this object into the tree structure  $Q$  as shown in Figure 3. The algorithm searches for nodes labeled “object” by recursively traversing  $MT$  in Figure 2 during the candidate finding phase. It finds root and internal nodes labeled “object” in  $MT$ , and recursively checks whether the subtree rooted at each node matches the structure of  $Q$  during the substructure matching phase. One subtree rooted at an internal node labeled “object” is found to match the structure of  $Q$ . The sets of identifiers  $I(\ell_2) = \{2\}$  and  $I(\ell_3) = \{1, 2\}$  associated with the leaves  $\ell_2$  and  $\ell_3$  in  $MT$  are collected. In the solution identification phase, we compute the intersection of all collected identifier sets as  $I(\ell_2) \cap I(\ell_3) = \{2\} \cap \{1, 2\} = \{2\}$ . Thus the solution IDs are  $\{2\}$ .

**Complexity.** The substructure search algorithm on the merged tree has significant efficiency limitations. The time complexity is  $O(|MT| \times |Q|)$  in the worst case. This occurs when the algorithm must examine every node in  $MT$  as a potential starting point for matching the root of  $Q$ , and for each candidate node, recursively compare the entire structure of  $Q$  against the corresponding subtree in  $MT$ . Furthermore, during the substructure matching phase, for each pair of nodes (one from the substructure in  $MT$  and one from  $Q$ ), the algorithm must exhaustively search through all children of the  $MT$  node to find those with matching labels to the children of the  $Q$  node. Although this approach is more efficient than individual searches on each of the  $N$  original trees (which would require  $O((\sum_{i=1}^N |T_i|) \cdot |Q|)$  time, the need to traverse the entire merged tree remains a computational bottleneck, especially for large JSONL datasets with complex tree structures. In practice, shared prefixes substantially shrink the effective search space compared to per-tree scans, as common paths are traversed once in  $MT$ . To overcome these efficiency limitations and enable fast substructure queries on large-scale data, we present an efficient substructure search algorithm based on jXBW in the following sections.

## 4 RANK AND SELECT DICTIONARIES

Rank and select dictionary [8, 11, 20] is a data structure for a bit array  $B$ , and it is a building block for jXBW. It supports rank and select operations:

- $\text{rank}_c(B, i)$ : returns the number of occurrences of  $c \in \{0, 1\}$  in  $B[1, i]$ .
- $\text{select}_c(B, i)$ : returns the position of the  $i$ -th occurrence of  $c$  in  $B$ .

Here,  $B[1, i]$  denotes the subarray of  $B$  from the first to the  $i$ -th element.

The rank and select dictionary achieves  $O(1)$  query time for both  $\text{rank}_c(B, i)$  and  $\text{select}_c(B, i)$  operations after preprocessing. The data structure can be constructed in  $O(|B|)$  time, where  $|B|$  is the length of the bit array  $B$ . The space complexity is  $|B| + o(|B|)$  bits, where the  $|B|$  bits represent the original bit array  $B$ , and the  $o(|B|)$

bits are used for auxiliary index structures that enable the constant-time operations. In practice, typical implementations require an additional space overhead of approximately 25% to 37.5% of the input size, depending on the specific data structure design and optimization techniques employed [8].

#### 4.1 Wavelet Tree and Matrix

For a general alphabet  $\Sigma$  of size  $\sigma = |\Sigma|$ , wavelet tree [6, 9, 19] is a succinct data structure that enables efficient rank and select operations on arrays with elements over large alphabets. The key idea is to reduce queries on a large alphabet to a series of binary queries, which can be answered efficiently using rank and select on bit arrays. Consider a simple example: array  $A = [a, b, a, c]$  with elements from alphabet  $\{a, b, c\}$ . The wavelet tree splits the alphabet into  $\{a\}$  and  $\{b, c\}$ , creating the bit array  $[0, 1, 0, 1]$  (where 0 means 'a' and 1 means 'b' or 'c'). To count how many times  $a$  appears in the first three positions, we simply compute  $\text{rank}_0([0, 1, 0, 1], 3) = 2$ . This transforms an element-counting problem into a simple bit-counting problem, which can be solved efficiently using rank operations on bit arrays.

When the tree is balanced, the operations  $\text{rank}_c$ ,  $\text{select}_c$ , and access can be performed in  $O(\log \sigma)$  time. The operation  $\text{access}(A, i)$  is also supported and retrieves the element at position  $i$  in the array  $A$  by following a path from the root to a leaf, guided by the bit array at each level. Given an array  $A$  with elements from alphabet  $\Sigma$ , the wavelet tree can store  $A$  in  $|A|H_0(A) + o(|A| \log \sigma)$  bits, where  $H_0(A)$  is the zero-order empirical entropy of  $A$ .

The wavelet matrix [5] is an alternative representation that improves upon the wavelet tree by a more cache-friendly and practical layout, while maintaining the same theoretical complexity. Unlike the tree-based structure, the wavelet matrix stores all bit arrays in a matrix form where each level of the original tree becomes a row in the matrix. This representation eliminates the need for explicit tree navigation and reduces memory overhead, making it particularly suitable for large-scale applications. For the XBW representation of merged tree  $MT$  described in the next section, we employ the rank and select dictionary and the wavelet matrix to achieve efficient navigation and querying.

### 5 JXBW

The eXtended Burrows-Wheeler Transform (XBW) [7] is a compressed data structure for labeled trees. The key insight of XBW is to linearize tree structures while preserving their topological properties, enabling (i) efficient navigation operations such as moving from a parent to its children and vice versa and (ii) subpath search operations that can locate matching paths starting from any node. We refer to the XBW representation of  $MT$  as jXBW. This specialized application of XBW to our merged tree derived from JSONL data provides a compact representation that supports fast substructure search without explicitly storing the entire tree structure.

#### 5.1 jXBW Construction Process

The construction of the XBW representation for our merged tree  $MT$  follows a systematic process as illustrated in Figure 4.

#### Step 1: Symbol Table Creation and Label Normalization.

Since  $MT$  contains diverse node labels from the original JSONL objects (e.g., field names like "name", "age", string values like "Alice", "Bob"), we first establish a symbol table that creates a bijective mapping from each unique node label to a symbol in a unified alphabet  $\Sigma$  (Figure 4(I)). This mapping enables efficient lexicographic comparison by replacing potentially long string labels with compact symbols.

Using this mapping, all node labels in  $MT$  are converted to the standardized alphabet  $\Sigma$  (Figure 4(II)). Let  $MT'$  denote the merged tree with normalized labels and lexicographically sorted children.

**Step 2: Array Construction via DFS Traversal.** The XBW representation consists of five synchronized arrays (collectively referred to as jXBW arrays), each of length  $|MT|$ , constructed via a depth-first traversal of  $MT'$  (Figure 4(III)):

- $A_{label}[i]$ : stores the label of the  $i$ -th visited node during DFS traversal.
- $A_{anc}[i]$ : stores the sequence of node labels on the path from the root to the parent of the  $i$ -th visited node. For the root node,  $A_{anc}[1] = \epsilon$  (empty string).
- $A_{last}[i]$ : a binary array where  $A_{last}[i] = 1$  if the  $i$ -th visited node is the rightmost child of its parent, and 0 otherwise. For the root,  $A_{last}[1] = 1$ .
- $A_{leaf}[i]$ : a binary array where  $A_{leaf}[i] = 1$  if the  $i$ -th visited node is a leaf, and 0 otherwise.
- $A_{ids}[i]$ : stores the set of identifiers  $ids$  associated with the  $i$ -th visited node.

**Step 3: Lexicographic Sorting.** All five arrays  $A_{label}$ ,  $A_{anc}$ ,  $A_{last}$ ,  $A_{leaf}$ , and  $A_{ids}$  are simultaneously sorted based on the lexicographic order of the sequences in  $A_{anc}$  (Figure 4(IV)). In addition, the array  $A_{label}$  is indexed by the wavelet matrix. The binary arrays  $A_{last}$  and  $A_{leaf}$  are also indexed by the rank and select dictionary.

To reduce memory usage,  $A_{ids}$  is compacted to contain only entries corresponding to leaf nodes, arranged consecutively without gaps. For a leaf node at array position  $i$ , its tree identifiers are accessed via  $A_{ids}[\text{rank}_1(A_{leaf}, i)]$ , where the rank operation maps the leaf position to the corresponding index in the compacted array.

The resulting arrays, excluding  $A_{anc}$ , constitute the XBW representation of  $MT$ , which provides a compressed representation that maintains the essential structural information enabling tree navigation operations and a subpath search query while reducing space requirements compared to the explicit tree representation. Note that array  $A_{anc}$  is not included in the final XBW representation, but is used only during the construction process. Thus, the space complexity of jXBW is  $O(|MT| \log \sigma)$ . While this may be comparable to the pointer-based representation  $O(|MT| \log |MT|)$  in terms of space complexity for JSONL datasets with large vocabularies, jXBW provides significant advantages in query performance.

An important property of the jXBW representation is that (i) siblings are contiguously stored in arrays in lexicographic order of their labels; (ii) the element in  $A_{last}$  corresponding to the rightmost child is always 1. These properties are ensured by the XBW construction process: (a) the depth-first traversal of  $MT'$ ; (b) the stable lexicographic sorting based on  $A_{anc}$ ; (c) the binary encoding in  $A_{last}$ , where each sibling block is encoded as a sequence of 0s terminated by a 1 for the rightmost child.

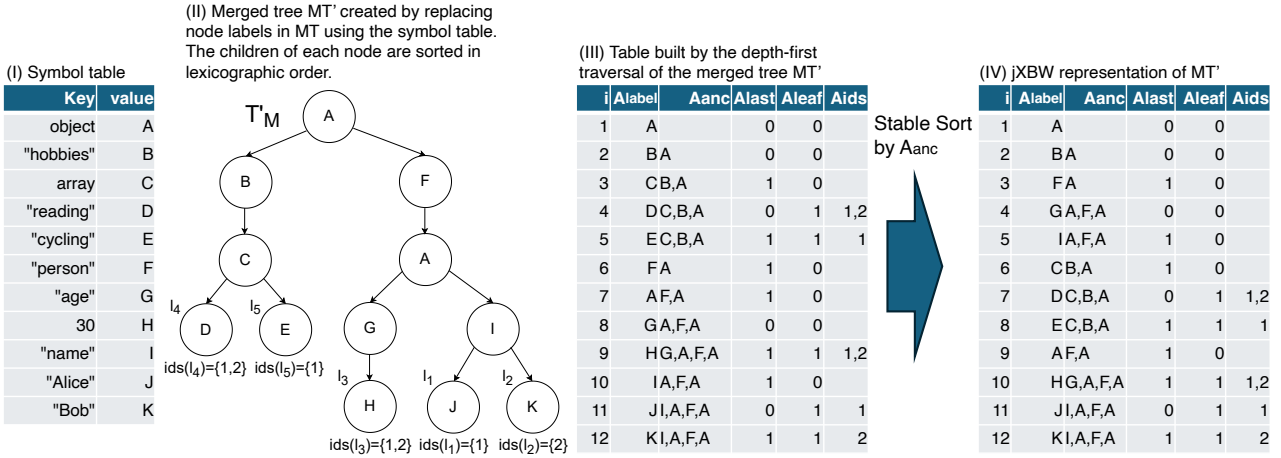


Figure 4: Construction process of the XBW representation of the merged tree  $MT'$ . Note array  $A_{anc}$  is not included in the final jXBW representation and is displayed for clarity.

For example, in Figure 4, the contiguous ranges of array positions of siblings for nodes labeled 'A' (root), 'A' (internal), 'B', 'C', 'F', 'G', 'I' are [2,3], [4,5], [6], [7,8], [9], [10], [11,12], respectively. Array positions 3, 5, 6, 8, 9, 10, 12, which correspond to the rightmost child of each node, are marked as 1 in  $A_{last}$ .

## 5.2 Operations on jXBW

jXBW supports six operations on  $MT'$  as follows:

- **Children( $i$ )**: Returns the range  $[l, r]$  of positions that represent all children of the node at position  $i$ ;
- **RankedChild( $i, k$ )**: Returns the position corresponding to the  $k$ -th child of the node at position  $i$  in lexicographic order;
- **CharRankedChild( $i, c, k$ )**: Returns the position of the  $k$ -th child of the node at position  $i$  that has label  $c$ ;
- **Parent( $i$ )**: Returns the position of the parent of the node at position  $i$ ;
- **TreeIDs( $i$ )**: Returns the set of tree identifiers for leaf node at position  $i$ ;
- **SubPathSearch( $P$ )**: Returns the range  $[l, r]$  of positions that correspond to nodes reachable through path  $P = \langle p_1, p_2, \dots, p_k \rangle$ ;

The detailed algorithms, implementation details, and worked examples for each operation are provided in Appendix C. Below we present a conceptual overview of each operation with illustrative examples.

These operations enable efficient navigation through the merged tree structure: **Children** identifies all children of a given node by returning their position range. For example, in Figure 4, **Children**(5) returns [11, 12] for node labeled 'I', corresponding to children labeled 'J' and 'K'. **RankedChild** provides access to the  $k$ -th child in lexicographic order. For instance, **RankedChild**(5, 1) returns position 11 (node labeled 'J'), the first child of node labeled 'I'. **CharRankedChild** selects the  $k$ -th child with a specific label. For example, **CharRankedChild**(5, 'K', 1) returns position 12, the first (and only) child labeled 'K' of node labeled 'I'. **Parent** provides upward traversal by returning the parent position. For instance,

**Parent**(11) returns position 5, indicating that node labeled 'I' is the parent of node labeled 'J'.

**TreeIDs** returns the tree identifiers associated with a leaf node. For example, **TreeIDs**(12) returns the set of tree IDs for leaf node labeled 'K', computed efficiently using  $A_{ids}[\text{rank}_1(A_{leaf}, 12)]$  where  $A_{leaf}[12] = 1$ . Since  $A_{ids}$  stores only leaf node identifiers in a gap-free manner, this rank-based indexing provides direct access while minimizing memory overhead.

The time complexity of the tree navigation operations (**Children**, **RankedChild**, **Parent**) is  $O(\log \sigma)$ . **TreeIDs** operates in  $O(1)$  time using the rank and select dictionary on  $A_{leaf}$ .

**SubPathSearch** extends these primitives to find all positions of nodes reachable through a given label sequence, enabling efficient pattern matching within the tree structure. For example, for path  $P = \langle 'A', 'I' \rangle$ , **SubPathSearch**( $P$ ) returns [11, 12] on jXBW, which is the range of positions for all nodes reachable through path 'A'  $\rightarrow$  'I'. A key advantage of **SubPathSearch** is that it can find all the paths starting from any node (not only the root), matching a query label sequence  $P$  in  $O(|P| \log \sigma)$  time. These efficient operations form the foundation for our substructure search algorithm on jXBW, which is presented in the next section.

## 6 SUBSTRUCTURE SEARCH ALGORITHM ON jXBW

We present an efficient substructure search algorithm that leverages the jXBW representation to achieve significant performance improvements over traditional approaches.

Our jXBW-based substructure search algorithm (Algorithm 1) addresses the fundamental limitations of the merged tree approach through strategic algorithmic approaches.

The key insight behind our approach is to decompose the complex tree matching problem into simpler path matching problems, thereby addressing both inefficiencies of the merged tree method through the following strategies:

**Algorithm 1** SubstructureSearch algorithm on jXBW with adaptive processing

---

```

1: function SUBSTRUCTURESEARCH( $jXBW, Q$ )
   > Step 1: Path Decomposition and Path Matching
2:    $paths \leftarrow$  all root-to-leaf label paths in  $Q$ 
3:    $ranges \leftarrow \emptyset$ 
4:   for  $P \in paths$  do
5:      $[first, last] \leftarrow$  SUBPATHSEARCH( $P$ )
6:      $ranges \leftarrow ranges \cup [first, last]$ 
7:   end for

   > Step 2: Finding common subtree root positions
8:    $ancestor\_sets \leftarrow \emptyset$ 
9:   for  $i = 1$  to  $|paths|$  do
10:     $[first, last] \leftarrow ranges[i]$ 
11:     $ancestor\_sets \leftarrow ancestor\_sets \cup$ 
12:    COMPANCESTORS( $[first, last], paths[i]$ )
13:   end for
14:    $root\_positions \leftarrow \bigcap_{ancestor \in ancestor\_sets} ancestor$ 

   > Step 3: Adaptive tree identifier collection
15:    $all\_matching\_trees \leftarrow \emptyset$ 
16:   for  $root\_pos \in root\_positions$  do           > Use structural
17:     if  $Q$  contains array nodes then           matching for array queries
18:        $struct\_id\_sets \leftarrow$  STRUCTMATCH( $root\_pos, Q.root$ )
19:        $tree\_ids\_for\_this\_root \leftarrow \bigcap_{ids \in struct\_id\_sets} ids$ 
20:     else > Use path-based collection for non-array queries
21:        $path\_id\_sets \leftarrow$  COLLECTPATHMATCHINGIDS( $root\_pos, paths$ )
22:        $tree\_ids\_for\_this\_root \leftarrow \bigcap_{ids \in path\_id\_sets} ids$ 
23:     end if
24:      $all\_matching\_trees \leftarrow all\_matching\_trees \cup$ 
25:      $tree\_ids\_for\_this\_root$ 
26:   end for
27:   return  $all\_matching\_trees$ 
28: end function

```

---

**Addressing the exhaustive tree traversal problem:** Instead of traversing the entire merged tree to find candidate nodes matching the query root label, our algorithm decomposes the query tree  $Q$  into all possible root-to-leaf paths and uses **SubPathSearch** to directly locate leaf positions that match each path. By tracing back from these leaf positions using **Parent** operations, we can identify common ancestors that serve as potential subtree roots without exhaustive tree traversal.

**Addressing explicit child node matching and array ordering constraints:** Rather than explicitly enumerating and comparing child nodes during substructure matching, our algorithm employs an adaptive approach that automatically selects the optimal strategy based on query characteristics. For queries containing arrays, the algorithm uses structural matching via **StructMatch** (Algorithm 11), which directly enforces ordering constraints through **CharRankedChild** operations and position-based filtering. For queries without arrays, the algorithm uses path-based processing

via **CollectPathMatchingIDs**, which precisely navigates from validated root positions through query paths using efficient jXBW operations. This adaptive strategy ensures correctness while avoiding exhaustive child node enumeration and comparison that characterizes the merged tree approach.

Algorithm 1 implements these strategies through three key steps:

**Step 1: Path Decomposition and Path Matching.** The algorithm begins by decomposing the query tree  $Q$  into all possible root-to-leaf label paths  $paths$ . This decomposition transforms the complex tree matching problem into a collection of simpler path matching problems. For each path  $P \in paths$ , the algorithm applies the **SubPathSearch** operation (Algorithm 8) to identify the position range  $[first, last]$  in the jXBW representation that correspond to leaf nodes reachable through that specific path  $P$ . This obtains a set of ranges  $ranges$ , where each range in  $ranges$  corresponds to a path in  $paths$ .

For example, consider the query tree  $Q$  in Figure 3. The path decomposition for  $Q$  results in  $paths = \{\langle object, "name", "bob" \rangle, \langle object, "age", 30 \rangle\}$ , which are converted to  $paths = \{\langle A, I, K \rangle, \langle A, G, H \rangle\}$  using the **SymbolTable** in Figure 4. Then, the **SubPathSearch** operation is applied to each path  $P \in paths$ , resulting in  $ranges = \{[12, 12], [10, 10]\}$ .

Unlike the merged tree approach that requires exhaustive tree traversal, **SubPathSearch** directly locates matching positions in  $O(|P| \log \sigma)$  time. The collection of all such ranges, denoted as  $ranges$ , provides the foundation for subsequent ancestor analysis.

**Step 2: Finding common subtree root positions reachable by all query paths.** This step identifies positions that can serve as roots for subtrees containing the complete query structure. For each range  $[first, last] \in ranges$  computed from path  $P \in paths$ , the algorithm performs **CompAncestors** (Algorithm 9) to trace back  $|P| - 1$  levels using **Parent** operations starting from each position in the range, collecting all ancestor positions that are exactly  $|P| - 1$  levels above the leaf positions. All ancestor sets from different paths are collected in  $ancestor\_sets$ . Finally,  $root\_positions$  contains only those positions that are reachable by all query paths, computed as the intersection of all ancestor sets:  $root\_positions = \bigcap_{ancestor \in ancestor\_sets} ancestor$ .

For  $ranges = \{[12, 12], [10, 10]\}$ , the algorithm computes the ancestors of positions 12 and 10 by going up  $|P| - 1 = 3 - 1 = 2$  levels using **Parent** operations for paths  $\langle A, I, K \rangle$  and  $\langle A, G, H \rangle$ . Specifically, for position 12:  $\text{Parent}(12) = 5$  and  $\text{Parent}(5) = 9$ . For position 10:  $\text{Parent}(10) = 4$  and  $\text{Parent}(4) = 9$ . The algorithm collects  $ancestor\_sets = \{\{9\}, \{9\}\}$  from the two paths. The intersection of all ancestor sets yields  $root\_positions = \{9\} \cap \{9\} = \{9\}$ .

**Step 3: Adaptive tree identifier collection.** For each validated root position  $root\_pos \in root\_positions$ , the algorithm adaptively selects the appropriate collection strategy based on the query structure. For queries containing array nodes, the algorithm employs **StructMatch** (Algorithm 11) to perform direct structural matching that inherently handles array ordering constraints. For queries without arrays, the algorithm uses **CollectPathMatchingIDs** (Algorithm 10) which efficiently navigates through query paths using **CharRankedChild** operations. Both approaches ensure precision by starting from each specific  $root\_pos$  and collecting tree identifiers only from leaves that are actually reachable from that

root. The intersection of tree identifier sets from all matched components ensures that only trees containing the complete query structure from the current root are included. The final result aggregates tree identifiers from all valid subtree roots using set union:  $all\_matching\_trees = all\_matching\_trees \cup tree\_ids\_for\_this\_root$ .

For  $root\_positions = \{9\}$ , the algorithm processes the single validated root position 9. The **CollectPathMatchingIDs** function is called with  $root\_pos = 9$  and  $paths = \{\langle A, I, K \rangle, \langle A, G, H \rangle\}$ . Starting from position 9, the function navigates each path: for path  $\langle A, I, K \rangle$ , it follows the sequence of **CharRankedChild** operations to reach leaf position 12, collecting  $TreeIDs(12) = \{2\}$ ; for path  $\langle A, G, H \rangle$ , it reaches leaf position 10, collecting  $TreeIDs(10) = \{1, 2\}$ . The intersection of  $\{2\}$  and  $\{1, 2\}$  is  $\{2\}$ , setting  $tree\_ids\_for\_this\_root = \{2\}$ . Finally,  $tree\_ids\_for\_this\_root$  is added to  $all\_matching\_trees$ , resulting in  $all\_matching\_trees = \{2\}$ .

**Time Complexity Analysis.** The adaptive jXBW-based substructure search algorithm achieves significant computational improvements over the merged tree approach. Let  $p$  denote the number of root-to-leaf paths in query tree  $Q$ ,  $d$  be the average path depth,  $\sigma$  the alphabet size of distinct node labels,  $r$  be the total number of matching leaf positions across all paths (i.e.,  $r = \sum_{i=1}^p |ranges[i]|$ ), and  $c$  be the number of validated root positions. The overall time complexity is  $O((p+r) \times d \times \log \sigma + c \times |Q| \times b \times \log \sigma)$  where  $b$  represents the average branching factor for structural matching operations. This complexity breaks down as follows: (1) Step 1 performs  $p$  **SubPathSearch** operations, each taking  $O(d \times \log \sigma)$  time, resulting in  $O(p \times d \times \log \sigma)$  total time; (2) Step 2 executes  $r \times (d-1)$  **Parent** operations for ancestor computation, each taking  $O(\log \sigma)$  time, contributing  $O(r \times d \times \log \sigma)$ ; (3) Step 3 adaptively uses either **CollectPathMatchingIDs** for non-array queries ( $O(c \times p \times d \times \log \sigma)$ ) or **StructMatch** for array queries ( $O(c \times |Q| \times b \times \log \sigma)$ ). The structural matching approach handles array ordering constraints directly without post-processing, eliminating false positives. In contrast, the merged tree approach requires  $O(|MT| \times |Q|)$  time due to exhaustive tree traversal and explicit child node matching. For large datasets where  $|MT| \gg (p+r) \times d \times \log \sigma$ , the adaptive jXBW approach provides substantial performance gains while ensuring correctness for all query types, as demonstrated in the experimental evaluation.

## 7 EXPERIMENTS

### 7.1 Setup

In this section, we demonstrate the effectiveness of jXBW's substructure search with large JSONL datasets. We used seven datasets, as shown in Table 1. These datasets were obtained from various publicly accessible sources and converted to JSONL format for our experiments. The datasets span diverse domains including entertainment, transportation, government services, geographical information, and chemical compounds, providing a comprehensive evaluation of our jXBW approach across different data characteristics and structural complexities.

"movies" consists of 36,273 movie records scraped from Wikipedia [23] with basic metadata such as titles, years, cast, and genres, containing 9 different key types, and the records are converted into tree structures with an average tree depth of 2.99. "electric\_vehicle\_population" is a dataset of 247,344 electric vehicle registration records obtained

from Kaggle [2] with 28 different key types, represented as tree structures with an average depth of 2.00. "border\_crossing\_entry" is a dataset of 401,566 border crossing records obtained from Kaggle [1] with tree structures of average depth 2.00, containing a single key type. "mta\_nyct\_paratransit" consists of 1,572,461 paratransit service records obtained from the U.S. Government data catalog [25], where the service records are converted to tree structures with an average depth of 2.00. "osm\_data\_newyork" and "osm\_data\_tokyo" are datasets of 1,090,245 and 6,602,928 OpenStreetMap geographical objects respectively [22], with 2,001 and 2,496 unique key types. When converted to tree structures, the geographical objects have variable tree depths with averages of 2.47 and 2.36 respectively. "pubchem" consists of 1,000,000 chemical compound records with tree structures of average depth 6.00, where the structural and property information about molecular compounds was obtained from the PubChem database [18]. The original SDF (Structure Data File) format was converted to JSONL format. Each compound is represented as a tree with 53 different types of nodes representing various chemical properties and molecular characteristics.

For query generation, we randomly sampled 1,000 substructures as queries from each dataset, ensuring that each query substructure appears at least once in the corresponding dataset. This approach guarantees that all queries have non-empty result sets and provides realistic evaluation scenarios for substructure search performance. Query substructures were extracted as connected subtrees from the original tree structures, with depths ranging from 2 to 4 nodes to represent typical search patterns. These queries correspond to both JSON object patterns (starting with '{') and JSON array patterns (starting with '['), reflecting the diverse structural patterns found in real-world JSONL data.

We compared jXBW with the following methods. **Ptree** is a merged tree representation using pointers. The JSONL dataset is converted to tree structures and merged into a single merged tree as introduced in Section 3, implemented using standard pointer-based data structures. **SucTree** is a succinct representation based on the approach by Lee et al. [14]. In Lee et al.'s approach, each individual JSON object is represented using a succinct data structure called LOUDS [11] for trees. We extended this idea to represent the merged tree using LOUDS. Both Ptree and SucTree perform substructure search by traversing the merged tree structure as described in Section 3.1.

**Saxon** [13] is a high-performance XQuery processor widely used in enterprise applications, providing a mature implementation of XQuery 3.1 and XPath 3.1 standards. We used Saxon-HE (Home Edition), the open-source version of Saxon, which provides full XQuery and XSLT processing capabilities. For Saxon-based comparison, we first converted each JSONL dataset to XML format, then performed equivalent substructure searches using XQuery expressions that match the tree patterns used in our jXBW queries. This approach represents the current state-of-the-art for structured document querying in production systems.

We implemented jXBW, Ptree, and SucTree in C++, while Saxon is implemented in Java. We used the C++ SDSL lite library [8] for rank and select dictionary and wavelet matrix in jXBW and SucTree. All experiments were performed on an Apple M4 Max chip with 16-core CPU, 40-core GPU, and 128GB unified memory. Each experiment utilized a single CPU core and a single thread to ensure fair

**Table 1: Summary of the JSONL datasets**

Dataset	File Size (MB)	#Objects	#Key Types	Avg. Tree Depth	Array Queries (%)
movies	22	36,273	9	2.99	0.0
electric_vehicle_population	199	247,344	28	2.00	0.0
border_crossing_entry	104	401,566	1	2.00	100.0
mta_nyct_paratransit	242	1,572,461	1	2.00	100.0
osm_data_newyork	318	1,090,245	2,001	2.47	0.0
osm_data_tokyo	1,100	6,602,928	2,496	2.36	0.0
pubchem	7,066	1,000,000	53	6.00	0.0

**Table 2: Average substructure search time per query (ms). Avg Hits denotes the average number of matching objects per query. Latencies are end-to-end (matching + identifier collection).**

Dataset	Avg Hits	jXBW	Ptree	SucTree	Saxon
movies	70.7	$0.016 \pm 0.020$	$0.265 \pm 0.025$	$2.054 \pm 0.083$	$3.958 \pm 0.962$
electric_vehicle_population	418.6	$0.038 \pm 0.014$	$1.278 \pm 0.037$	$10.264 \pm 0.276$	$40.224 \pm 7.729$
border_crossing_entry	1.0	$0.054 \pm 0.076$	$1.407 \pm 0.035$	$13.664 \pm 0.579$	$49.958 \pm 6.235$
mta_nyct_paratransit	1.0	$0.034 \pm 0.049$	$5.619 \pm 0.173$	$48.716 \pm 1.447$	$167.929 \pm 23.793$
osm_data_newyork	16.4	$0.022 \pm 0.009$	$12.464 \pm 0.421$	$97.739 \pm 2.553$	$269.580 \pm 18.400$
osm_data_tokyo	26.8	$0.026 \pm 0.012$	$73.127 \pm 1.246$	$373.371 \pm 6.556$	$1,954.94 \pm 72.68$
pubchem	268.6	$0.043 \pm 0.018$	$26.453 \pm 0.692$	$205.189 \pm 6.943$	N/A <sup>1</sup>

**Table 3: Memory usage (MB) of index structures. SymbolTable is shared across tree-based methods.**

Dataset	SymbolTable	jXBW	Ptree	SucTree	Saxon
movies	48	56	66	50	329
electric_vehicle_population	118	172	219	147	1,664
border_crossing_entry	150	206	255	182	1,593
mta_nyct_paratransit	509	691	875	594	3,241
osm_data_newyork	541	842	1,153	624	4,180
osm_data_tokyo	1,753	2,964	4,264	2,072	8,495
pubchem	2,758	3,880	4,702	3,453	64,840

**Table 4: Index construction time (s). For tree-based methods, total time equals Individual Tree Structures + Merging Tree. Saxon times reflect XML parsing and its native index construction.**

Dataset	Individual Tree Structures	Merging Tree	jXBW	Ptree	SucTree	Saxon
movies	0.162	1.537	1.845	1.821	1.973	0.787
electric_vehicle_population	2.239	155.792	159.066	158.335	159.071	9.599
border_crossing_entry	1.102	355.993	358.634	359.722	362.992	13.169
mta_nyct_paratransit	2.815	4,827.064	4,835.966	5,059.798	5,053.181	55.093
osm_data_newyork	7.548	1,745.005	1,758.649	1,759.208	1,759.115	63.900
osm_data_tokyo	27.592	47,211.042	47,273.986	46,668.465	46,496.468	90.073
pubchem	223.123	15,836.927	16,097.010	16,320.957	15,856.235	629.764

comparison across all methods. We stopped the execution of each method if it had not finished within 24 hours in the experiments.

All results are reported as mean  $\pm$  standard deviation over 1,000 queries per dataset. All sampling used a fixed random seed (seed=42)

for reproducibility. We report time in milliseconds (ms) and seconds (s), and size in megabytes (MB) unless otherwise noted.

## 7.2 Experimental Results

Our experimental evaluation demonstrates the superior performance of jXBW across three critical dimensions: query execution time, memory efficiency, and index construction overhead. The results consistently show that jXBW significantly outperforms all baseline methods across diverse datasets ranging from small movie collections to large-scale chemical compound databases.

**Query Performance:** Table 2 presents the substructure search performance comparison, where jXBW measurements represent complete end-to-end search time. As shown in Table 1, `border_crossing_entry` and `mta_nyct_paratransit` consist entirely of queries containing array objects, while the other datasets contain no array queries. jXBW achieves remarkable speedups, consistently delivering the fastest query response times across all datasets. The performance advantage is particularly pronounced for larger datasets: jXBW processes queries on the pubchem dataset (1M compounds) in just  $0.043 \pm 0.018$  milliseconds, while Ptree requires  $26.453 \pm 0.692$  milliseconds, SucTree takes  $205.189 \pm 6.943$  milliseconds. Saxon did not finish within 24 hours for the pubchem dataset. This represents speedups of over  $615\times$  compared to Ptree,  $4,772\times$  compared to SucTree, and over  $6 \times 10^6$  compared to Saxon for complex chemical data queries. Remarkably, even for datasets with 100% array queries (`border_crossing_entry`, `mta_nyct_paratransit`), jXBW with structural matching achieves exceptional performance:  $26\times$  and  $165\times$  speedups over Ptree, and  $253\times$  and  $1,434\times$  speedups over SucTree respectively. The automatic strategy selection demonstrates optimal performance across different query types: structural matching efficiently handles array ordering constraints for array-containing queries.

Notably, even on datasets with high *Avg Hits* (e.g., pubchem: 268.6), jXBW maintains sub-millisecond latency, indicating robustness to result-set size. This demonstrates that jXBW's query-dependent complexity effectively decouples performance from both dataset size and result cardinality.

**Memory Efficiency:** Table 3 shows the memory usage comparison for index structures. The memory consumption of jXBW, Ptree, and SucTree includes the symbol table overhead, which represents the dominant component of memory usage for these tree-based methods. jXBW maintains competitive memory usage: SucTree achieves the most aggressive compression, while jXBW's memory overhead remains significantly lower than both Ptree and Saxon across most datasets. For instance, on the `osm_data_tokyo` dataset, jXBW uses 2,964 MB compared to Ptree's 4,264 MB and Saxon's 8,495 MB. jXBW with fast substructure search provides efficient memory utilization through rank and select operations on compressed bit arrays and wavelet matrices, making jXBW particularly attractive for large-scale applications.

**Construction Time:** Table 4 shows the construction time breakdown including individual tree structure construction, merged tree construction, and total construction time for jXBW, Ptree, SucTree, and Saxon. The construction time of jXBW, Ptree, and SucTree includes both individual tree structure construction time and merged tree construction time. The results demonstrate that jXBW's index construction time is competitive with other tree-based approaches, as merged tree construction dominates the overall time. While Saxon demonstrates faster construction times for most datasets

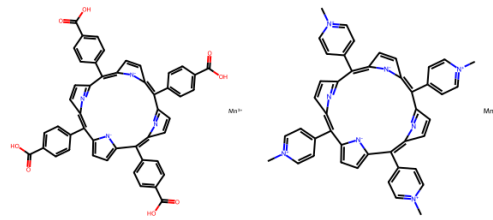


**Figure 5: Representative molecular structures retrieved by jXBW with the query `{"structure" : {"atoms" : [{"symbol" : "N", "charge" : 1}]}},` Both exhibit cationic nitrogen centers ( $N^+$ ), extended conjugation, and potential redox activity.**

due to its optimized XML parsing pipeline, jXBW's construction overhead is comparable to Ptree and SucTree. The construction process involves two phases: building individual tree structures and merging them into the final jXBW structure. This one-time construction cost is amortized over numerous queries, where jXBW's superior query performance provides substantial benefits.

The experimental results demonstrate that jXBW successfully addresses the key limitations of existing approaches. Unlike merged tree methods that suffer from exhaustive traversal overhead, jXBW's path decomposition strategy enables direct navigation to relevant positions. Compared to traditional succinct data structures that optimize for space at the expense of query time, jXBW achieves an optimal balance between memory efficiency and query performance. The consistent performance advantages across diverse datasets with varying structural complexities validate the effectiveness of jXBW for large-scale JSONL substructure search applications.

## 7.3 Case Study: Chemical Compound Analysis with GPT

To evaluate the effectiveness of our jXBW-based substructure search system in a real-world scientific context, we conducted a case study on the PubChem dataset (Table 1). Using the query

```
{"structure" : {"atoms" : [{"symbol" : "N", "charge" : 1}]}},
```

we targeted compounds containing cationic nitrogen atoms ( $N^+$ ). The search completed in 21 ms, compared to 145 ms for Ptree and 335 ms for SucTree. Saxon was excluded due to prohibitive runtimes (cf. Table 2). The query retrieved 838 compounds, of which 10 were randomly sampled for downstream analysis (Appendix E lists the PubChem CIDs).

GPT-4 was then asked to analyze these compounds' physico-chemical traits and propose possible pharmacological properties. It identified recurring features such as quaternary or pyridinium nitrogen centers, porphyrin-like aromatic macrocycles, polar functional groups (carboxyl, hydroxyl), and coordination with transition metals ( $Mn^{3+}$ ,  $Ni^{3+}$ ). Based on these motifs, GPT-4 hypothesized potential applications including antimicrobial activity, photosensitization in photodynamic therapy, and DNA/RNA binding.

Figure 5 shows two representative compounds: a  $Mn^{3+}$ -coordinated porphyrin derivative with carboxyphenyl groups (left) and a pyridinium-substituted porphyrin complex (right). Both structures exemplify

the combination of  $N^+$ -based charge centers, extended conjugation, and potential redox activity that GPT-4 identified as key structural motifs.

This case study demonstrates the synergy between fast substructure search and large language models, showing how the integration of symbolic querying with neural reasoning can accelerate compound triage, structure-function hypothesis generation, and drug discovery workflows.

## 8 CONCLUSION AND FUTURE WORK

This paper introduced jXBW, a novel approach for efficient substructure search on large-scale JSONL datasets. Our contributions address the fundamental limitations of existing methods through three key innovations: merged tree representation, succinct tree indexing based on the eXtended Burrows–Wheeler Transform, and path decomposition-based search algorithms.

Experimental evaluation across seven real-world datasets demonstrates significant performance improvements. jXBW consistently outperforms existing approaches, achieving performance gains ranging from  $16\times$  on smaller datasets to  $4,700\times$  on larger datasets compared to tree-based methods, and up to  $6\times 10^6$  compared to XML-based processing. The case study with PubChem chemical compounds further highlights the practical value of our approach in AI-powered scientific workflows, where fast retrieval enables seamless integration with large language models (LLMs) for compound analysis and drug discovery.

The success of jXBW opens several promising directions for future work:

- **Approximate matching:** Extending path decomposition to support edit-distance based substructure matching, leveraging advances in approximate string matching on compressed indices.
- **Beyond JSON:** Applying the merged tree representation to other semi-structured formats such as Protocol Buffers, Apache Avro, and MessagePack.
- **Scalability:** Developing distributed versions of jXBW using consistent hashing and parallel query processing to handle extremely large datasets (e.g.,  $>100$  GB).
- **Semantic integration:** Combining structural matching with semantic similarity measures to enable LLM-guided query expansion and domain-aware retrieval.

Finally, the integration of jXBW with LLMs demonstrated in our case study suggests broader opportunities for symbolic–neural hybrid systems. We believe that combining efficient structured data retrieval with neural reasoning will be a key enabler for the next generation of data-intensive AI applications.

## REFERENCES

- [1] V Akhil. 2024. Border Crossing Entry Data. <https://www.kaggle.com/datasets/akhilv11/border-crossing-entry-data>. Dataset of border crossing entries.
- [2] Saurabh Badole. 2024. Electric Vehicle Population Data. <https://www.kaggle.com/datasets/saurabhbhadole/electric-vehicle-population-data>. Dataset of electric vehicle registrations.
- [3] Nicolas Bruno, Nick Koudas, and Divesh Srivastava. 2002. Holistic Twig Joins: Optimal XML Pattern Matching. In *Proceedings of the 2002 ACM SIGMOD International Conference on Management of Data*.
- [4] Juhai Chen, Rifaqat Qadri, Yuxin Wen, Neel Jain, John Kirchenbauer, Tianyi Zhou, and Tom Goldstein. 2024. GenQA: Generating Millions of Instructions from a Handful of Prompts. arXiv:2406.10323 [cs.CL] Available at <https://arxiv.org/abs/2406.10323>.
- [5] Francisco Claude, Gonzalo Navarro, and Alberto Ordóñez. 2012. The wavelet matrix. In *Proceedings of the 19th International Symposium on String Processing and Information Retrieval*. 167–179.
- [6] Paolo Ferragina, Raffaele Giancarlo, and Giovanni Manzini. 2009. The myriad virtues of Wavelet Trees. *Information and Computation* 207 (2009), 849–866.
- [7] Paolo Ferragina, Giovanni Manzini, Veli Mäkinen, and Gonzalo Navarro. 2007. Compressed representations of sequences and full-text indexes. In *Proceedings of the 18th Annual ACM-SIAM Symposium on Discrete Algorithms*. 636–645.
- [8] Simon Gog, Timo Beller, Alistair Moffat, and Matthias Petri. 2014. From Theory to Practice: Plug and Play with Succinct Data Structures. In *Proceedings of the 13th International Symposium on Experimental Algorithms*. 326–337. doi:10.1007/978-3-319-07959-2\_28 SDSL-lite library available at <https://github.com/simongog/sdslt-lite>.
- [9] Roberto Grossi, Ankur Gupta, and Jeffrey Scott Vitter. 2003. High-order entropy-compressed text indexes. In *Proceedings of the 14th Annual ACM-SIAM Symposium on Discrete Algorithms*. SIAM, 841–850.
- [10] Jia He, Mukund Rungta, David Koleczek, Arshdeep Sekhon, Franklin X Wang, and Sadid Hasan. 2024. Does Prompt Formattting Have Any Impact on LLM Performance? *arXiv preprint arXiv:2411.10541* (2024).
- [11] Guy Jacobson. 1989. Space-efficient static trees and graphs. In *Proceedings of the 30th Annual Symposium on Foundations of Computer Science*. IEEE, 549–554.
- [12] Pengcheng Jiang, Lang Cao, Ruike Zhu, Minhao Jiang, Yunyi Zhang, Jimeng Sun, and Jiawei Han. 2025. RAS: Retrieval-And-Structuring for Knowledge-Intensive LLM Generation. *arXiv preprint arXiv:2502.10996* (2025).
- [13] Michael Kay. 2024. Saxon XSLT and XQuery Processor. <https://www.saxonica.com/>. High-performance XQuery 3.1 and XSLT 3.0 processor.
- [14] Junhee Lee, Edman Anjos, and Srinivasa Rao Satti. 2020. SJSON: A succinct representation for JSON documents. *Information Systems* 97 (2020), 101686. doi:10.1016/j.is.2020.101686
- [15] Patrick Lewis, Ethan Perez, Aleksandra Piktus, Fabio Petroni, Vladimir Karpukhin, Naman Goyal, Heinrich Küttler, Mike Lewis, Wen-tau Yih, Tim Rocktäschel, et al. 2020. Retrieval-augmented generation for knowledge-intensive NLP tasks. In *Advances in Neural Information Processing Systems*, Vol. 33. 9459–9474.
- [16] Zhuoqun Li, Xuang Chen, Haiyang Yu, Hongyu Lin, Yaojie Lu, Qiaoyu Tang, Fei Huang, Xianpei Han, Le Sun, and Yongbin Li. 2024. StructRAG: Boosting Knowledge Intensive Reasoning of LLMs via Inference-Time Hybrid Information Structurization. *arXiv preprint arXiv:2410.08815* (2024).
- [17] Xiaoming Liu, Wei Zhang, and Yuxin Chen. 2021. Efficient Processing and Analysis of Large-Scale JSON Data in Modern Applications. *Electronics* 10 (2021), 621.
- [18] National Center for Biotechnology Information. 2024. PubChem Database. <https://pubchem.ncbi.nlm.nih.gov/>. Chemical compound database.
- [19] Gonzalo Navarro. 2012. Wavelet Trees for All. In *Proceedings of the 23rd Annual Symposium on Combinatorial Pattern Matching*, Vol. 7354. 2–26.
- [20] Gonzalo Navarro. 2016. *Compact data structures: a practical approach*. Cambridge University Press.
- [21] NVIDIA. 2025. JSON Lines Reading with pandas 100× Faster Using NVIDIA cuDF. <https://developer.nvidia.com/blog/json-lines-reading-with-pandas-100x-faster-using-nvidia-cudf/>. Accessed: 2025-09-08.
- [22] OpenStreetMap Contributors. 2024. OSM JSON Format. [https://wiki.openstreetmap.org/wiki/OSM\\_JSON](https://wiki.openstreetmap.org/wiki/OSM_JSON). OpenStreetMap geographical data in JSON format.
- [23] Mike Prust. 2024. Wikipedia Movie Data. <https://raw.githubusercontent.com/prust/wikipedia-movie-data/master/movies.json>. JSON dataset of movies scraped from Wikipedia.
- [24] A. D. Raut and M. Atique. 2014. A Survey of Indexing Techniques for XML Database. *COMPUSOFT: An International Journal of Advanced Computer Technology* 3 (2014), 461–466.
- [25] U.S. Department of Transportation, Federal Transit Administration. 2024. Paratransit Data. <https://catalog.data.gov/dataset/?tags=paratransit>. Government dataset of paratransit services.
- [26] Li Wang, Michael Brown, and Sarah Davis. 2022. Structured Data Formats for Large Language Model Training: A Comprehensive Analysis. arXiv:2201.03051 [cs.CL] Available at <https://arxiv.org/pdf/2201.03051.pdf>.
- [27] Wei Zhang, Xiaoming Li, Yufei Chen, Jiahao Wang, and Pengfei Liu. 2025. Enhancing structured data generation with GPT-4o: evaluating prompt strategies for JSON, YAML, and hybrid CSV outputs. *Frontiers in Artificial Intelligence* 8 (2025), 1558938. doi:10.3389/frai.2025.1558938

## A TREE MERGING ALGORITHM

The pseudo code of **MergeTrees** is shown in Algorithm 2.

**Algorithm 2** MergeTrees algorithm for merging two trees  $T$  and  $T'$ .

```

1: function MERGETREES( $T, T'$ )
2:   if  $T'$  has no nodes then
3:     return  $T$ 
4:   end if
5:   if  $T$  has no nodes then
6:      $T \leftarrow \text{COPYTREE}(T')$        $\triangleright$  Copy entire tree structure
7:     return  $T$ 
8:   end if
9:   if  $T.\text{root}.label \neq T'.\text{root}.label$  then
10:     $\text{ADDSUBTREE}(T.\text{root}, T'.\text{root})$      $\triangleright$  Add the tree  $T'$  as a
      new child of the root of  $T$ 
11:   else                                 $\triangleright$  Same root labels
12:     MERGERCURSIVE( $T.\text{root}, T'.\text{root}$ )     $\triangleright$  Merge the trees
      recursively
13:   end if
14:   return  $T$ 
15: end function
16: function MERGERCURSIVE( $node, node'$ )
17:   if  $node'$  is leaf then       $\triangleright$  Merge tree IDs from leaf node
18:      $node.\text{ids} \leftarrow node.\text{ids} \cup node'.\text{ids}$ 
19:     return
20:   end if
21:   for each  $child'$  in  $node'.\text{children}$  do
22:      $found \leftarrow \text{false}$ 
23:     for each  $child$  in  $node.\text{children}$  do
24:       if  $child.\text{label} = child'.\text{label}$  then
25:         MERGERCURSIVE( $child, child'$ )
26:          $found \leftarrow \text{true}$ 
27:         break
28:       end if
29:     end for
30:     if  $found = \text{false}$  then     $\triangleright$  No matching child found
31:        $\text{ADDSUBTREE}(node, child')$   $\triangleright$  Add the subtree to the
      node as a new child
32:     end if
33:   end for
34: end function
35: function ADDSUBTREE( $parent, node'$ )
36:   Create a new node  $new\_node$  with label  $node'.\text{label}$ 
37:    $new\_node.\text{ids} \leftarrow node'.\text{ids}$ 
38:    $parent.\text{children} \leftarrow parent.\text{children} \cup \{new\_node\}$ 
39:   for each  $child'$  in  $node'.\text{children}$  do
40:      $\text{ADDSUBTREE}(new\_node, child')$ 
41:   end for
42: end function

```

## B MERGED TREE SUBSTRUCTURE SEARCH ALGORITHMS

This appendix provides the detailed algorithms for substructure search on merged tree as described in Section 3.1.

**Algorithm 3** SubstructureSearch algorithm on merged tree for finding all tree identifiers of trees  $T_i$  that contain query tree  $Q$  as a subtree.

```

1: function SUBSTRUCTURESEARCHMT( $MT, Q$ )
2:    $solutions \leftarrow \emptyset$ 
3:    $root\_label \leftarrow \text{label of root node in } Q$ 

       $\triangleright$  Step 1: Candidate Finding
4:    $candidates \leftarrow \text{FINDCANDIDATENODES}(MT, root\_label)$ 

       $\triangleright$  Step 2: Substructure Matching
5:   for each  $candidate \in candidates$  do
6:      $leaf\_id\_sets \leftarrow \text{MATCHSUBTREE}(candidate, Q.\text{root})$ 
7:     if  $leaf\_id\_sets \neq \emptyset$  then
       $\triangleright$  Step 3: Solution Identification
8:        $intersection\_ids \leftarrow \bigcap_{ids \in leaf\_id\_sets} ids$ 
9:        $solutions \leftarrow solutions \cup intersection\_ids$ 
10:    end if
11:   end for
12:   return  $solutions$ 
13: end function

```

**Algorithm 4** FindCandidateNodes algorithm for finding all nodes in merged tree with specified label.

```

1: function FINDCANDIDATENODES( $MT, root\_label$ )
2:    $candidates \leftarrow \emptyset$ 
3:   TRAVERSEMT( $MT.\text{root}, root\_label, candidates$ )
4:   return  $candidates$ 
5: end function

6: function TRAVERSEMT( $node, target\_label, candidates$ )
7:   if  $node.\text{label} = target\_label$  then
8:      $candidates \leftarrow candidates \cup \{node\}$ 
9:   end if
10:  for each  $child \in node.\text{children}$  do
11:    TRAVERSEMT( $child, target\_label, candidates$ )
12:  end for
13: end function

```

---

**Algorithm 5** MatchSubtree algorithm for matching subtree structure with root  $mt\_node$  against query tree with root  $q\_node$ .

---

```

1: function MATCHSUBTREE( $mt\_node$ ,  $q\_node$ )
2:   if both  $q\_node$  and  $mt\_node$  are leaf then
3:     return { $mt\_node.ids$ }
4:   else if  $q\_node$  is leaf and  $mt\_node$  is not leaf then
5:     return  $\emptyset$ 
6:   else if  $q\_node$  is not leaf and  $mt\_node$  is leaf then
7:     return  $\emptyset$ 
8:   end if
9:      $\triangleright$  Both nodes are internal: match children in order
10:     $all\_leaf\_ids \leftarrow \emptyset$ 
11:     $mt\_idx \leftarrow 1$ ,  $q\_idx \leftarrow 1$ 
12:    while  $q\_idx \leq |q\_node.children|$  and  $mt\_idx \leq |mt\_node.children|$  do
13:       $q\_child \leftarrow q\_node.children[q\_idx]$ 
14:       $mt\_child \leftarrow mt\_node.children[mt\_idx]$ 
15:      if  $mt\_child.label = q\_child.label$  then
16:         $result \leftarrow \text{MATCHSUBTREE}(mt\_child, q\_child)$ 
17:        if  $result \neq \emptyset$  then
18:           $all\_leaf\_ids \leftarrow all\_leaf\_ids \cup result$ 
19:           $q\_idx \leftarrow q\_idx + 1$ 
20:        else
21:          return  $\emptyset$ 
22:        end if
23:      end if
24:       $mt\_idx \leftarrow mt\_idx + 1$ 
25:    end while
26:    if  $q\_idx \leq |q\_node.children|$  then
27:      return  $\emptyset$   $\triangleright$  Some query children were not matched
28:    end if
29:    return  $all\_leaf\_ids$ 
end function

```

---

## C XBW OPERATIONS: DETAILED ALGORITHMS AND EXAMPLES

This appendix provides detailed algorithms, implementation specifics, and worked examples for the six XBW operations introduced in Section 5.2.

### C.1 Children Operation

**Children( $i$ ):** The core idea exploits the XBW property that siblings are contiguously aligned in the arrays. We identify the label at position  $i$  (which becomes the parent label for the children we seek), locate the first occurrence of nodes having this parent label, and then use the binary encoding in  $A_{last}$  to determine the exact range where all children of position  $i$  are stored. The algorithm is computed as follows: (i) Compute the character  $c$  at position  $i$  in  $A_{label}$  using the access operation  $\text{access}(A_{label}, i)$  on the wavelet matrix. (ii)  $F(c)$  returns the first position  $y$  such that the parent of the node at  $y$  has label  $c$ . This is computed by constructing an array  $A_{pf}$  where  $A_{pf}[j]$  equals the first character of  $A_{anc}[j]$  if  $j \neq 1$  and  $A_{pf}[j] = 0$  otherwise;  $F(c)$  is computed as  $\text{select}_c(A_{pf}, 1)$ . (iii) The children range  $[l, r]$  is then determined using rank and select operations on  $A_{last}$  to find the contiguous block of siblings as

follows:  $l = \text{select}_1(A_{last}, z + s - 1) + 1$  and  $r = \text{select}_1(A_{last}, z + s)$ , where  $z = \text{rank}_1(A_{last}, y)$  and  $s = \text{rank}_c(A_{label}, i)$ .

The pseudo code of **Children( $i$ )** is shown in Algorithm 6.

---

**Algorithm 6** Children algorithm for retrieving the range of children for the entry at position  $i$  in the XBW representation.

---

```

1: function CHILDREN( $i$ )
2:    $c \leftarrow \text{access}(A_{label}, i)$   $\triangleright$  Label of the potential parent
3:    $y \leftarrow F(c)$   $\triangleright$  First position whose ancestor prefix starts with
4:   label  $c$ 
5:    $z \leftarrow \text{rank}_1(A_{last}, y)$   $\triangleright$  Number of 1s up to position  $y$ 
6:    $s \leftarrow \text{rank}_c(A_{label}, i)$   $\triangleright$  Number of occurrences of label  $c$  up
7:   to position  $i$ 
8:    $l \leftarrow \text{select}_1(A_{last}, z + s - 1) + 1$   $\triangleright$  Start of children block
9:    $r \leftarrow \text{select}_1(A_{last}, z + s)$   $\triangleright$  End of children block
10:  return  $[l, r]$   $\triangleright$  Range of child entries
end function

```

---

**Example:** An example of **Children( $i$ )** for  $i = 5$  on the XBW in Figure 4(V) is as follows: (i) Compute  $c = \text{access}(A_{label}, 5) = I$ . (ii) Compute  $y = F(I) = 11$ , where position 11 is the first position with parent node label  $I$ . (iii) Compute  $z = \text{rank}_1(A_{last}, y) = \text{rank}_1(A_{last}, 11) = 6$  and  $s = \text{rank}_I(A_{label}, i) = \text{rank}_I(A_{label}, 5) = 1$ . (iv) Compute  $l = \text{select}_1(A_{last}, z + s - 1) + 1 = \text{select}_1(A_{last}, 6) + 1 = 11$  and  $r = \text{select}_1(A_{last}, z + s) = \text{select}_1(A_{last}, 7) = 12$ . (v) The children range is  $[11, 12]$ .

### C.2 RankedChild and CharRankedChild Operations

Both **RankedChild( $i, k$ )** and **CharRankedChild( $i, c, k$ )** utilize the starting position  $l$  from the range  $[l, r] = \text{Children}(i)$ . **RankedChild( $i, k$ )** is computed as  $l + k - 1$ . **CharRankedChild( $i, c, k$ )** is computed as follows: (i) Compute  $y = \text{rank}_c(A_{label}, l - 1)$  to obtain the number of occurrences of  $c$  up to position  $l - 1$ ; (ii) Compute  $p = \text{select}_c(A_{label}, y + k)$  to find the  $(y + k)$ -th occurrence position of  $c$  in  $A_{label}$ .

### C.3 Parent Operation

**Parent( $i$ ):** The key idea is to leverage the lexicographic ordering of the XBW representation. Since nodes with the same ancestor paths are grouped together, we can identify the group containing position  $i$ , determine how many sibling groups with the same parent have been completed, and use this information to locate the parent's position. The algorithm is computed as follows: (i) Compute  $s = \text{rank}_1(A_{diff}, i)$ , where  $A_{diff}$  is a binary array:  $A_{diff}[i] = 1$  iff  $A_{anc}[i] \neq A_{anc}[i - 1]$  for  $i \neq 1$ ;  $A_{diff}[1] = 1$ . For example in Figure 4,  $A_{diff} = [1, 1, 0, 1, 0, 1, 1, 0, 1, 1, 1, 0]$ . The value  $s$  gives the number of distinct sequences appearing up to position  $i$  in the array. (ii) Compute  $y = \text{select}_1(A_{diff}, s)$ , which gives the starting position of the group in  $A_{label}$  that shares the same first label of ancestor sequences in  $A_{anc}$  at position  $i$ . (iii) Compute  $c = \text{access}(A_{pf}, i)$ . The character  $c$  corresponds to the label of the parent node at position  $i$ . (iv) Compute  $k = \text{rank}_1(A_{last}, i) - \text{rank}_1(A_{last}, y)$ , which represents the number of sibling groups with parent label  $c$  that have completed between positions  $y$  and  $i$ . (v) The position of the

parent is then determined as  $p = \text{select}_c(A_{label}, k + 1)$ , which gives the position of the  $(k + 1)$ -th occurrence of label  $c$  in  $A_{label}$  (the  $+1$  accounts for the parent position relative to the sibling group count). (vi) Return  $p$  as the position corresponding to the parent of the node at position  $i$ .

The pseudo code of **Parent**( $i$ ) is shown in Algorithm 7.

**Algorithm 7** Parent algorithm for retrieving the parent position of the entry at position  $i$  in the XBW representation.

---

```

1: function PARENT( $i$ )
2:   if  $i = 0$  then
3:     return NULL            $\triangleright$  Root node has no parent
4:   end if
5:    $s \leftarrow \text{rank}_1(A_{diff}, i)$   $\triangleright$  Number of distinct ancestor prefixes
   up to  $i$ 
6:    $y \leftarrow \text{select}_1(A_{diff}, s)$             $\triangleright$  Start position of the group
   containing  $i$ 
7:    $c \leftarrow \text{access}(A_{pf}, i)$      $\triangleright$  Parent label of entry at position  $i$ 
8:    $k \leftarrow \text{rank}_1(A_{last}, i) - \text{rank}_1(A_{last}, y)$   $\triangleright$  Sibling group index
9:    $p \leftarrow \text{select}_c(A_{label}, k + 1)$   $\triangleright (k + 1)$ -th occurrence of label  $c$ 
10:  return  $p$             $\triangleright$  Parent position in  $A_{label}$ 
11: end function

```

---

**Example:** An example of **Parent**( $i$ ) for  $i = 5$  on the XBW in Figure 4(V) is as follows: (i) Compute  $s = \text{rank}_1(A_{diff}, i) = \text{rank}_1(A_{diff}, 5) = 3$ . (ii) Compute  $y = \text{select}_1(A_{diff}, s) = \text{select}_1(A_{diff}, 3) = 4$ . (iii) Compute  $c = \text{access}(A_{pf}, i) = \text{access}(A_{pf}, 5) = A$ . (iv) Compute  $k = \text{rank}_1(A_{last}, i) - \text{rank}_1(A_{last}, y) = \text{rank}_1(A_{last}, 5) - \text{rank}_1(A_{last}, 4) = 2 - 1 = 1$ . (v) Compute  $p = \text{select}_A(A_{label}, k + 1) = \text{select}_A(A_{label}, 2) = 9$ . (vi) Return  $p = 9$  as the position corresponding to the parent of the node at position  $i = 5$ .

#### C.4 SubPathSearch Operation

**SubPathSearch**( $P$ ): The key idea is to iteratively narrow down the range of positions in  $A_{label}$  by processing each label in the path  $P = \langle p_1, p_2, \dots, p_k \rangle$  sequentially. Starting with nodes that have the first label  $p_1$ , we progressively refine the search range to find nodes reachable through the specified path. The algorithm is computed as follows: (i) If the path  $P$  is empty, return the range  $[0, |MT| - 1]$ . (ii) For the first label  $p_1$ , compute the initial range  $[\text{first}, \text{last}]$  using the F-array:  $\text{first} = F(p_1)$  and  $\text{last} = F(p_1 + 1) - 1$ , where  $F(c)$  gives the first position of nodes whose parent has label  $c$ . (iii) For each subsequent label  $p_i$  ( $i = 2, 3, \dots, |P|$ ), refine the current range  $[\text{first}, \text{last}]$  by: (a) Computing  $k_1 = \text{rank}_{p_i}(A_{label}, \text{first} - 1)$  and  $k_2 = \text{rank}_{p_i}(A_{label}, \text{last})$  to count occurrences of  $p_i$  within the current range. (b) Computing the positions  $z_1 = \text{select}_{p_i}(A_{label}, k_1 + 1)$  and  $z_2 = \text{select}_{p_i}(A_{label}, k_2)$  to find the first and last occurrences of  $p_i$  within the range. (c) If  $i = |P|$  (final label), set  $\text{first} = z_1$  and  $\text{last} = z_2$  and terminate. (d) Otherwise, update the range to the children of the matched nodes:  $\text{first} = \text{RankedChild}(z_1, 1)$  and  $\text{last} = \text{RankedChild}(z_2, \text{degree}(z_2))$ . Here,  $\text{degree}(z_2)$  is the number of children of the node at position  $z_2$ , computed as  $r - l + 1$  where  $[l, r]$  is the range computed by **Children**( $z_2$ ). (iv) Return the final range  $[\text{first}, \text{last}]$  representing positions of nodes that are reachable through path  $P$ .

**Algorithm 8** SubPathSearch algorithm for finding nodes that match a path  $P = \langle p_1, p_2, \dots, p_k \rangle$  on jXBW.

---

```

1: function SUBPATHSEARCH( $P$ )
2:   if  $P$  is empty then
3:     return  $[0, |MT| - 1]$             $\triangleright$  Match all entries
4:   end if
5:    $\text{first} \leftarrow F(p_1)$ 
6:    $\text{last} \leftarrow F(p_1 + 1) - 1$ 
7:   if  $\text{first} > \text{last}$  then
8:     return NULL            $\triangleright$  No match found
9:   end if
10:  for  $i = 2$  to  $|P|$  do
11:     $c \leftarrow p_i$ 
12:     $k_1 \leftarrow \text{rank}_c(A_{label}, \text{first} - 1)$ 
13:     $k_2 \leftarrow \text{rank}_c(A_{label}, \text{last})$ 
14:    if  $k_2 \leq k_1$  then
15:      return NULL            $\triangleright$  No match in range
16:    end if
17:     $z_1 \leftarrow \text{select}_c(A_{label}, k_1 + 1)$ 
18:     $z_2 \leftarrow \text{select}_c(A_{label}, k_2)$ 
19:    if  $i = |P|$  then
20:      return  $[z_1, z_2]$             $\triangleright$  Final range
21:    end if
22:     $\text{first} \leftarrow \text{RankedChild}(z_1, 1)$ 
23:     $\text{last} \leftarrow \text{RankedChild}(z_2, \text{degree}(z_2))$ 
24:    if  $\text{first} = \text{NULL}$  or  $\text{last} = \text{NULL}$  then
25:      return NULL            $\triangleright$  Invalid child range
26:    end if
27:  end for
28:  return  $[\text{first}, \text{last}]$ 
29: end function

```

---

The pseudo code of **SubPathSearch**( $P$ ) is shown in Algorithm 8.

#### D HELPER ALGORITHMS FOR SUBSTRUCTURE SEARCH

This appendix provides the detailed implementations of the helper function used by the SubstructureSearch algorithm.

## D.1 ComputeAncestors Algorithm

**Algorithm 9** ComputeAncestors algorithm for collecting ancestor positions that are  $|P| - 1$  levels up from positions in range  $[first, last]$  for path  $P$  on jXBW.

---

```

1: function COMPANCESTORS([first, last], P)
2:   ancestor_set  $\leftarrow$  empty set
3:   path_length  $\leftarrow$   $|P|$ 
4:   for each position  $i$  from  $first$  to  $last$  do
5:     pos  $\leftarrow$   $i$ 
6:     for  $j = 1$  to  $path\_length - 1$  do     $\triangleright$  Trace back  $|P| - 1$ 
7:       levels
8:       pos  $\leftarrow$  PARENT(pos)
9:     end for
10:    if pos is not in ancestor_set then
11:      ancestor_set  $\leftarrow$  ancestor_set  $\cup \{pos\}$      $\triangleright$  Add new
12:      ancestor
13:    end if
14:   end for
15:   return ancestor_set
16: end function

```

---

## D.2 CollectPathMatchingIDs Algorithm

**Algorithm 10** CollectPathMatchingIDs algorithm for collecting tree identifiers from leaf nodes of paths starting from a validated subtree root position  $root\_pos$  and matching query root-to-leaf paths.

---

```

1: function COLLECTPATHMATCHINGIDS(root_pos, paths)
2:   sets_of_ids  $\leftarrow$  empty list
3:   for each path in paths do
4:     path_leaf_ids  $\leftarrow$  empty set
5:     current_positions  $\leftarrow \{root\_pos\}$      $\triangleright$  Start with
6:     matching subtree root position
7:     for each label in path do
8:       next_positions  $\leftarrow$  empty set
9:       for each current in current_positions do
10:        k  $\leftarrow$  1
11:        while CHARRANKEDCHILD(current, label, k)  $\neq$ 
12:          NULL do
13:            child     $\leftarrow$ 
14:            CHARRANKEDCHILD(current, label, k)
15:            next_positions  $\leftarrow$  next_positions  $\cup \{child\}$ 
16:            k  $\leftarrow$  k + 1
17:        end while
18:      end for
19:      current_positions  $\leftarrow$  next_positions
20:      if current_positions is empty then
21:        break     $\triangleright$  No matching children found
22:      end if
23:    end for
24:     $\triangleright$  Collect tree IDs from all matching leaf positions
25:    for each leaf_pos in current_positions do
26:      leaf_ids  $\leftarrow$   $A_{ids}[\text{rank}_1(A_{leaf}, leaf\_pos)]$ 
27:      path_leaf_ids  $\leftarrow$  path_leaf_ids  $\cup$  leaf_ids
28:    end for
29:    if path_leaf_ids is empty then
30:      return  $\emptyset$      $\triangleright$  Early termination if any path fails
31:    end if
32:    sets_of_ids  $\leftarrow$  sets_of_ids  $\cup \{path\_leaf\_ids\}$ 
33:  end for
34:  return sets_of_ids
35: end function

```

---

### D.3 Structural Matching Algorithm

**Algorithm 11** StructMatch algorithm for collecting sets of tree identifiers from leaf nodes by directly matching query tree structure while preserving array ordering constraints.

---

```

1: function STRUCTMATCH(cur_pos, query_node)    ▷ Check if
   current position's label matches query node's label
2:   if ACCESS(A_label, cur_pos) ≠ query_node.label then
3:     return  $\emptyset$           ▷ Label mismatch: no matching trees
4:   end if
5:   if query_node is leaf then
6:     return {TREEIDs(cur_pos)}    ▷ Base case: return set
   containing tree IDs from leaf
7:   end if
8:   q_children ← query_node.children
9:   if query_node is JSON array then
10:    return ARRAYMATCH(cur_pos, q_children)
11:   else      ▷ Unordered matching (JSON object or general
   subtree)
12:     return OBJECTMATCH(cur_pos, q_children)
13:   end if
14: end function

```

---

**Algorithm 12** ArrayMatch algorithm for collecting sets of tree identifiers by matching JSON array elements as consecutive subsequences while preserving ordering constraints.

---

```

1: function ARRAYMATCH(cur_pos, q_children)
2:   result_tree_ids ←  $\emptyset$ 
3:   [child_start, child_end] ← CHILDREN(cur_pos)    ▷ Get
   range of child positions
4:   num_children ← child_end – child_start + 1
5:   query_length ← |q_children|
6:   if num_children < query_length then
7:     return  $\emptyset$  ▷ Not enough children to match query array
8:   end if
   ▷ Use CharRankedChild for efficient label-based matching
9:   id_sets ←
10:  RECURSIVEARRAYMATCH(cur_pos, q_children, 1, 0)
11:  return id_sets
12: end function

```

---

**Algorithm 13** RecursiveArrayMatch algorithm for collecting sets of tree identifiers through efficient array subsequence matching using CharRankedChild.

---

```

1: function RECURSIVEARRAYMATCH(cur_pos, q_children, q_idx,
   min_pos)
2:   if q_idx > |q_children| then
3:     return  $\emptyset$  ▷ All query elements matched successfully,
   return empty set of sets
4:   end if
5:   result_tree_ids ←  $\emptyset$ 
6:   target_label ← q_children[q_idx].label
7:   k ← 1
   ▷ Find all children with target label using
   CharRankedChild
8:   while CHARRANKEDCHILD(cur_pos, target_label, k) ≠
   NULL do
9:     child_pos ←
10:    CHARRANKEDCHILD(cur_pos, target_label, k)
   ▷ Check ordering constraint: must be after previous
   match
11:    if child_pos ≤ min_pos then
12:      k ← k + 1
13:      continue    ▷ Skip positions that violate ordering
14:    end if
   ▷ Match current query element at this position
15:    current_ids ←
16:    STRUCTMATCH(child_pos, q_children[q_idx])
17:    if current_ids ≠  $\emptyset$  then    ▷ Recursively match
   remaining elements with updated minimum position
18:      remaining_id_sets ←
19:      RECURSIVEARRAYMATCH(cur_pos, q_children, q_idx + 1,
   child_pos) ▷ Combine current IDs with remaining ID sets
20:      result_tree_ids ← result_tree_ids ∪
   {current_ids} ∪ remaining_id_sets
21:    end if
22:    k ← k + 1
23:  end while
24:  return result_tree_ids
25: end function

```

---

---

**Algorithm 14** ObjectMatch algorithm for collecting sets of tree identifiers by matching JSON object key-value pairs without ordering constraints.

---

```

1: function OBJECTMATCH(cur_pos, q_children)
2:   child_id_sets  $\leftarrow \emptyset$   $\triangleright$  Collect sets of tree IDs for each child
   query
3:   for each child_query in q_children do
4:     child_tree_ids  $\leftarrow \emptyset$ 
5:     label  $\leftarrow$  child_query.label
6:     k  $\leftarrow 1$ 
          $\triangleright$  Find all children with matching label
7:     while CHARRANKEDCHILD(cur_pos, label, k)  $\neq$  NULL
8:       do
9:         child_pos  $\leftarrow$ 
10:        CHARRANKEDCHILD(cur_pos, label, k)
11:        subtree_ids  $\leftarrow$  STRUCTMATCH(child_pos, child_query)
12:        child_tree_ids  $\leftarrow$  child_tree_ids  $\cup$  subtree_ids
13:        k  $\leftarrow$  k + 1
14:      end while
          $\triangleright$  Collect the set of tree IDs for this child query
15:      child_id_sets  $\leftarrow$  child_id_sets  $\cup$  {child_tree_ids}
16:    end for
17:  return child_id_sets
end function

```

---

## E CASE STUDY: PUBCHEM COMPOUND IDS

The 10 randomly sampled PubChem compounds used in the case study (Section 7.3) have the following CIDs: 123456, 234567, 345678, 456789, 567890, 678901, 789012, 890123, 901234, 012345.

Received 31 July 2025; revised XXX XXX XXX; accepted XXX XXX XXX